Research Square

Preprints are preliminary reports that have not undergone peer review.
They should not be considered conclusive, used to inform clinical practice,
or referenced by the media as validated information.

Selenium Nanoparticle–2D Material Hybrid Composites for Redox Regulation in Saccharomyces cerevisiae: Biochemical and Microchemical Insights

Huma Gulzar
Harbin Institute of Technology
Asma Gulzar
Syracuse University
Iftikhar Ahmed
Abu Dhabi 11 University
Nawal Fatima
Abu Dhabi 11 University
Muhammad Zubair Nawaz
Southern University of Science and Technology
Xiaojun Han
Harbin Institute of Technology
Muhammad Saqib Saqib Saif
Manash Kozybayev North Kazakhstan University
Dmitriy Berillo
Manash Kozybayev North Kazakhstan University
Ghazala Mustafa
Quaid-i-Azam University
Murtaza Hasan
murtaza@iub.edu.pk

Islamia University of Bahawalpur

Research Article

Keywords: Selenium (Se), selenium nanoparticles (Se-NPs), Saccharomyces cerevisiae, green synthesis, glutathione redox cycle (GSH:GSSG)

Posted Date: November 10th, 2026

DOI: https://doi.org/10.21203/rs.3.rs-11123369/v1

License: This work is licensed under a Creative Commons Attribution 4.0 International License.
Read Full License

Additional Declarations: No competing interests reported.

Selenium Nanoparticle–2D Material Hybrid Composites for Redox Regulation in *Saccharomyces cerevisiae*: Biochemical and Microchemical Insights

Huma Gulzar[1], Asma Gulzar[2], Iftikhar Ahmed[3], Nawal Fatima[3], Muhammad Zubair Nawaz[4], Xiaojun Han[1*], Muhammad Saqib Saif[5], Dmitriy Berillo[5], Ghazala Mustafa[6], Murtaza Hasan[*7]

[1] School of Chemistry and Chemical Engineering, Harbin Institute of Technology, Harbin 150001, China.

[2]Department of Chemistry, Syracuse University, Syracuse, New York 13210, USA

[3]Environmental and Public Health Department, College of Health Science, Abu Dhabi 11 University P.O. Box 59911 Abu Dhabi, United Arab Emirates

[4]Laboratory of 2D Optoelectronics and Nanoelectronics (L2DON), Department of Materials Science amd Engineering, Southern University of Science and Technology, Shenzhen 518055 China

[5]Department of Chemistry and Chemical Technology, Manash Kozybayev North Kazakhstan University, 86, Pushkin Str., Petropavlovsk 150000, Kazakhstan

[6]Department of Plant Sciences, Faculty of Biological Sciences, Quaid-i-Azam University, Islamabad, Pakistan

[7]Department of Biotechnology, Faculty of Chemical and Biological Sciences, The Islamia University of Bahawalpur, Bahawalpur 63100, Pakistan

Corresponding Author*
Murtaza Hasan PhD
Department of Biotechnology, IBBB
Email: murtaza@iub.edu.pk

Abstract

Selenium serves as an essential element and recognizes as for its vital biological significance by acting as cofactor . Despite its essentiality, dual role of selenium as a beneficial micronutrient at optimal concentrations and a potential pro-oxidant at high concentrations under external stress remains a critical area of investigation in *Saccharomyces cerevisiae*. However, advent of redox homeostasis regulator and stress controller green synthesized selenium nanoparticles (Se-NPs) has emerged as a promising solution. The research examines the dose-dependent effects of Se-NPs on the growth dynamics and glutathione redox cycle (GSH:GSSG) in *Saccharomyces cerevisiae* subjected to external stress conditions. Synthesized Se-NPs were prepared and confirmed by Ultraviolet–visible (UV–Vis) spectra at peak at 300 nm. Scanning electron microscopy (SEM) showed a spherical with irregular patterns of Se-NPs. The analysis by energy-dispersive X-ray spectroscopy (EDS) revealed a strong intensity of Se as compared to other elements. Yeast culture was exposed to selenium treatments at different concentrations: No selenium (control), <0.1 mg/L, 0.1–1 mg/L, and >2 mg/L, with evaluations focusing on microscopic morphology, spectroscopic absorbance (A600), cell counts and the redox equilibrium of the GSH:GSSG cycle in mitochondria, cytosol and nucleus under external stress conditions, including thermal stress, ethanol stress, H_2O_2 stress (oxidative damage), and HU stress (replication disruption). Selenium dose at 0.1–1 mg/L improved cell viability together with stress tolerance by preserving a high GSH:GSSG ratio which promote antioxidant defense whereas excessive selenium dose (>2 mg/L) induced cytotoxicity and disrupted glutathione homeostasis leading to redox imbalance. These findings described a critical threshold for Se-NP bioactivity that identify its protective versus toxic effects. Understanding of selenium dose-dependent modulation in redox homeostasis provides fundamental insights into

the potential biotechnological, redox biology and therapeutic applications along with stress management strategies.

Keywords: **S**elenium (Se), selenium nanoparticles (Se-NPs), *Saccharomyces cerevisiae,* green synthesis, glutathione redox cycle (GSH:GSSG).

1. Introduction

An important micronutrient, selenium (Se) is vital for maintaining cellular homeostasis, especially in controlling oxidative stress, immunological responses, and enzymatic activity in living systems [1–3]. It is a critical constituent of selenoproteins, which are the part of glutathione (GSH) redox system such as glutathione peroxidase (GSH-Px) which protects cells by neutralizing lipid peroxides and hydrogen peroxides[4, 5] and thioredoxin reductase which maintains cellular redox potential[6]. These selenoproteins highlight selenium's function in sustaining cellular function under a variety of cellular environmental conditions by enabling adaptive responses to oxidative stress[7] and preserving mitochondrial and cytosolic redox states[8]. The glutathione (GSH) redox system acts as a protective buffer against reactive oxygen species (ROS) and serves as a crucial factor in determining cellular health under stress . One important indicator of redox balance is the ratio of reduced glutathione (GSH) to oxidized glutathione (GSSG), which represents the redox state of the cell[9]. This ratio controls signaling cascades essential for adaptation and survival under stress, affects metabolic pathways, and assesses the cell's ability to counteract oxidative stress [10]. Selenium supplementation enhance the activity of antioxidant enzymes such as glutathione reductase (GR) and glutathione peroxidase (GPx), which in turn modifies the GSH:GSSG cycle [11]. However, excessive reactive oxygen species (ROS) production [12], mitochondrial

dysfunction and disrupted cellular processes can result from an imbalance in selenium dosage, leading to oxidative damage[13, 14].

Currently, the most common forms of selenium added to feeds on the market are inorganic and organic selenium[15]. However, because of its high excretion in feces, inorganic Se has been criticized for its high toxicity and detrimental effects on the environment [16]. Organic Se is less harmful than inorganic Se; however, when organic diselenides, like selenocysteine and selenocystamine, are exposed to thiols, they transform into seleniums (RSeH), which also produce reactive oxygen species and oxidative stress [17]. Nanotechnological research studies have been conducted recently. People are more interested in using selenium nanoparticles (Se-NPs) trace elements as animal feed supplements because they are less toxic and have a higher bioavailability than inorganic salt [18]. Research has indicated that compared to other Se compounds (such as selenite, selenomethionine, and Se-methylselenocysteine), Se-NPs are less harmful to animals [19, 20]. Animals' growth performance, feed conversion rate, immunity, and capacity to withstand oxidative stress can be enhanced by adding Se-NPs to their diet. Se-NPs like other NPs has shown unique because of their redox characteristics, intrinsic antioxidant activity[21, 22], reduced toxicity[23], biocompatibility[24], and capability to alter intracellular signaling pathways[25]. The size and shape of NPs, such as silver , gold, iron, and Se-NPs, have a long-lasting connection with their unique properties, functions, and applications[26, 27]. In addition to being expensive, easily aggregated, and having unstable size and shape, chemical and physical methods of fabricating Se-NPs have many other drawbacks, including a complicated synthesis process[28, 29], a lack of environmental friendliness, and the need for strict conditions, which restricts the use of Se-NPs. As an alternative to chemical and physical methods, the green synthesis method for fabricating Se-NPs

from plant extracts is thought to be a viable substitute due to its narrow size and shape distribution, low toxicity, high stability, cost-effective and environmental friendly[30, 31]. In order to examine the nature of protein adsorption, scientists have also investigated into how Se-NPs interact with various biological fluids.

The goal of this study is to green synthesize and characterize the green-synthesized Se-NPs and to find its dose-dependent effect by investigating its role at varying concentrations in modulating growth and glutathione redox cycle in three different organelles, mitochondria, cytosol and nucleus of yeast exposed to external stress conditions such as a thermal, ethanol, hydrogen peroxide, and HU stressors. Additionally, deeper understanding of Se-NP biological significance insights its role in biotechnological applications by providing practical implications for optimizing selenium usage in enhancing yeast resilience in industrial fermentation processes particularly under oxidative and other environmental stress conditions.

2. Materials and Method

2.1 Experimental material

Yeast strain BY4741, peptone, glucose, yeast extract, sodium selenite (Na_2SeO_3), *C.sativus* tree leaves, TCA buffers, ethanol, hydrogen peroxide (H_2O_2), hydroxyurea (HU), ice-cold water, 1x PBS buffer, sucrose, HEPES, EDTA, Tris-HCl, NaCl, KCl, MgCl2, DTT, NP-40, PMSF, glass beads, Beutler's reagents, Habeeb's methods reagents and ultra-pure distilled water for washing purpose.

2.2 *C.sativus* extract preparation

The leaves of *C.sativus* tree were collected from the local area of Beijing. After thoroughly cleaning the leaves with tap water to get rid of any dirt, cleaned with distilled water, dried, and ground. 50 g powder was added to 100 mL of distilled water or acetone,

and the mixture was boiled for almost 50 minutes at 80 to 90 °C. The heated mixture was filtered through Whatman filter paper. Kept at 4 °C and used as a reducing agent [32]. The meticulous protocol made sure that the extract from *C.sativus* tree leaves reached the highest quality and was appropriately processed for use in further investigations or practical applications.

2.3 Preparation of Se-NPs

In a 250 mL reagent bottle, sodium selenite was mixed with 100 mL of double-distilled water to fabricate Se-NPs. Using a magnetic stirrer, the mixture was heated and stirred at 70–80 °C for one minute. Then mixture was then mixed with 20 mL of an aqueous solution of the *C.sativus* leaf extract, which was used as a reducing agent. After 15 minutes, 20 mL of sodium hydroxide aqueous solution (to maintain the pH of solution) was added with the ratio of 3 mL per minute. After a uniform precipitations, the Se-NPs were left to cool at room temperature. Se-NPs were obtained by decanting after 30 minutes, then washing three times with distilled water and once with ethanol. Then dried in an oven to obtain the powder of Se-NPs.

2.4 Treatments for interaction of yeast culture with Se-NPs

Saccharomyces cerevisiae BY4741 was the main experimental yeast strain, purchased from Open-biosystems. Yeast cells were grown at 30°C in YPD (1% yeast extract, 2% peptone, 2% glucose) liquid culturing medium (pH 5.5), in flask with liquid-to-air volume ratio of 1:5 at 200 rpm until it reached mid-log phase (OD600 ~0.6–0.8). Yeast strain was harvested by centrifugation at 6000 rpm for 1 minute and stored in the laboratory at−80 °C for further treatments.

The experiment used a completely randomized design with three replications for each treatment at 30°C. The following treatments were included in this experiment:

No Se-NPs (control)

<0.1 mg/L Se-NPs concentrations

0.1–1 mg/L Se-NPs concentrations

>2 mg/L Se-NPs concentrations

2.5 Yeast cultures and Se-NPs separation after incubation periods

After the completion of the incubation period, the yeast cultures and Se-NPs were separated. The samples were placed in a centrifuge machine and centrifuged for 5 minutes at 10,000 rpm. The NPs settled down at the bottom after 5 minutes of centrifugation, while yeast was present as a supernatant on the top. The Se-NPs in the bottom were then separated out and put in an incubator set to 70 °C for 15 minutes after being washed three times with distilled water and once with ethanol. Yeast cultures from each treatment after interaction with Se-NPs, were kept at -80 °C for further analysis. The yeast-treated dried Se-NPs were then ground into a fine powder and kept in the separated, labeled Eppendorf tubes for use in subsequent characterization [33].

2.6 Characterization of Se-NPs

A S22PC spectrophotometer was used to record the ultraviolet-visible (UV-Vis) absorption spectra of Se-NPs incubated with or without yeast cultures. This method involved measuring time by time spectra of the solution and periodically sampling aliquots to monitor yeast-treated Se-NPs. The UV spectrum of each aliquot was monitered as a function of time retention on the UV spectrophotometer, and these spectra were recorded every 30 minutes [34].

The morphology, texture, and element composition of both without or with yeast-treated Se-NPs were observed and detected through microscopic analysis using a scanning electron microscope (SEM, Talos 200 s, FEI, USA) equipped with energy dispersive X-ray spectroscopy (EDS)[2].

2.7 Morphological and growth assessment of yeast cultures

Microscopic observations were conducted by incubating yeast cells of different treatments for 24–48 hours to assess cellular morphology and identify potential selenium-induced structural changes in different organelles. Imaging was performed using a light microscope with DIC optics. Cells growth were monitored by measuring optical density (OD) at 600 nm (A600) using a spectrophotometer.

2.8 Cell proliferation

Cell counts were obtained using a hemocytometer. Proliferation rate was compared across different selenium treatment groups. The concentration of cells in each sample was calculated using the formula:

Cell concentration (cells/mL) = Average cell count per square×dilution factor/ chamber volume

2.9 Implication of stress conditions

To evaluate the different stress responses, yeast cells under different selenium treatments were subjected to the following stress conditions:

Thermal Stress: Cultures were exposed to 45°C (heat shock) and 10°C (cold shock).

Ethanol Stress: Ethanol was added to a final concentration of 10% (v/v).

Oxidative Stress: Cultures were treated with 2mM H_2O_2 for 30 minutes.

Replication Stress: Hydroxyurea (HU) was added to a final concentration of 10mM.

2.10 Mitochondrial isolation

Centrifugation at 4000×g for 5 minutes was used to harvest the yeast cells from all treatments and control. Washed pellet with ice-cold water (PBS buffer) to remove media components. Pellet was resuspended in a mitochondrial isolation buffer (250mM

sucrose, 10mM HEPES, pH 7.4, 1mM EDTA). Applied mechanical method to disrupt the cells like glass beads beating. Removed unbroken cells and debris by centrifuging at low speed (ie, 1000 × g). Supernatant collected, spun at higher speed (10,000×g for 15 min) in order to pellet the mitochondria. For further analysis, mitochondrial pellet was resuspended in a small volume of the isolation buffer[35].

2.11 Cytosol isolation

Centrifugation at 3000–4000×g for 5 minutes was used to harvest the yeast cells from all treatments and control. To remove residual media components, washed the pellet with ice cold water or 1x PBS buffer. After washing the yeast pellet, resuspended in a buffer for cytosol isolation (50mM Tris HCl, pH 7.5, 150mM NaCl, 1mM EDTA, protease inhibitors (PMSF)). Then we used the mechanical method to disrupt the cells by vortex in the presence of glass beads. Removed unbroken cells and debris (pellet) by centrifuging the lysate at 3,000–5,000×g for 10–15 minutes at 4° C. Transferred supernatant to a clean tube. This supernatant contained cytosolic fraction, used for further analysis .

2.12 Nuclear isolation

Centrifuged all treatments and control at 3000 to 4000xg for 5 minutes then harvested the yeast cells. To remove residual media components, washed the pellet with ice cold water or 1x PBS buffer. After washing the yeast pellet, resuspended in a buffer for nuclear isolation (20mM HEPES, pH 7.5, 10mM KCl, 2mM $MgCl_2$, 0.5mM DTT, 1mM EDTA, 0.5%NP-40) with protease inhibitors (PMSF)). Disrupted the cells by mechanical method without excessive shearing like beads beating. Then centrifuged the mixture at 1,000− 2,000xg for 5−10 minutes at 4°C to remove unbroken cells and large debris (pellet). Supernatant was transferred to a new tube and spun at 10,000×g for 20 minutes at 4°C. After this centrifugation, pellet contained the nuclear fraction and

supernatant contained the cytoplasmic components. To remove the cytoplasmic residuals, washed the nuclear pellet with nuclear isolation buffer. The nuclear pellet was resuspended in a small volume of ice cold buffer for further analysis .

2.13 Glutathione Determination

For a finding of glutathione, samples were suspended in the 10% TCA and vortexed for 10 min. Reduced glutathione (GSH) levels from each subcellular compartment were calculated in supernatant after centrifugation at 10,000 g for 30 min by using method of Beutler et al. (42). Habeeb's method was preferred to estimate the total glutathione content in each subcellular compartment (43). Oxidized glutathione (GSSG) levels from each subcellular compartment were calculated from the difference between the values of total glutathione content and reduced glutathione (GSH) levels.

2.14 Interpreting results

All the results were expressed as GSH:GSSG ratio. After quantifying the levels of GSH and GSSG in the mitochondrial, cytosol and nuclear fraction, calculated the GSH:GSSG ratio. The GSH concentration is divided by GSSG concentration and the GSH:GSSG ratio was obtained. High GSH:GSSG ratio suggested a reduced state in the mitochondria, cytosol and nucleus, while a low ratio suggested oxidative stress or a shift towards oxidative damage.

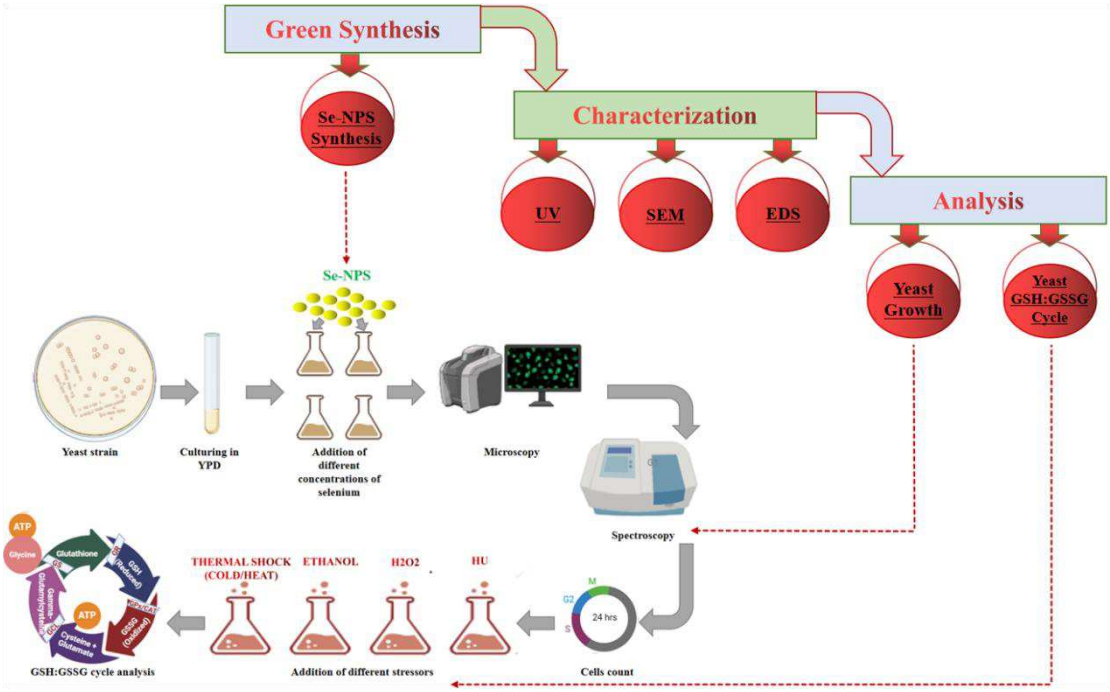
2.15 Statistical analysis

All the samples used in this research were in triplicate form and used statistical analysis for interpretation by calculating mean ± standard deviation (SD) and standard errors.

3. Results and Discussion

Immune regulative, anti-oxidative, environmental friendly and economical selenium nanoparticles (Se-NPs) with high stability and good bio-compatibility were prepared

by green chemistry method. The Se-NPs were well characterized by using modern techniques such as Ultra-visible spectrometry (UV–Vis spectrometry), scanning electron microscopy (SEM), and energy-dispersive X-ray spectroscopy (EDS). Different Se-NPs concentration treatments demonstrated a dose dependent effect on growth and GSH:GSSG cycle in three different sub-cellular compartments under various external stress conditions in *Saccharomyces cerevisiae.* A schematic representation (Scheme 1), proposed the Se-NPs synthesis, Se-NPs characterization and analysis process of yeast growth and yeast GSH:GSSG cycle.



Scheme 1. Overall experimental layout of Se-NPS synthesis, characterization to yeast growth analysis under different Se-NPs concentrations and yeast GSH:GSSG cycle.

3.1 Characterization of Se-NPs

Ultra-visible spectrometry (UV–Vis spectrometry) stands as an important method used for confirming the synthesis and stability of nanoparticles within aqueous solutions. In case of synthesizing Se-NPs from plant extract, the UV–Vis spectra revealed an exclusive surface plasmon resonance (SPR) band at the range of 200-500 nm wavelength as given in (Fig. 1a). Particularly, it was noted that after 1 h of the

reaction, the Se-NPs showed a SPR band with a wavelength of 300 nm. The reason for the slight change in each case is basically because of the change in concentration of particles as also reported[36].

Scanning electron microscopy (SEM) analysis was employed to validate the surface morphology, particle size, and dimensional characteristics of biologically synthesized Se-NPs, displayed a spherical-shaped irregular morphology of before and after yeast-treated Se-NPs in the treatment groups (Fig. 1b,c,d,e,f). Furthermore, energy-dispersive X-ray spectroscopy (EDS) spectrum of synthesized Se-NPs was performed to demonstrate the elemental composition and composition change of the product. From the spectrum image (Fig. 1g,h), it can be distinguished that Se is present at a strong intensity as compared to carbon and oxygen that are present at low intensity; hence, it shows the purity of Se-NPs, *i.e.*, free of impurities. These results also matched with previous investigation of researcher who synthesized Se-NPs by green chemistry methods. we can conclude that there is strong interaction between Se-NPs and yeast cultures for making distinction of nanoparticle characteristics between incubated and non-incubated nanoparticles also reported the same results[37].

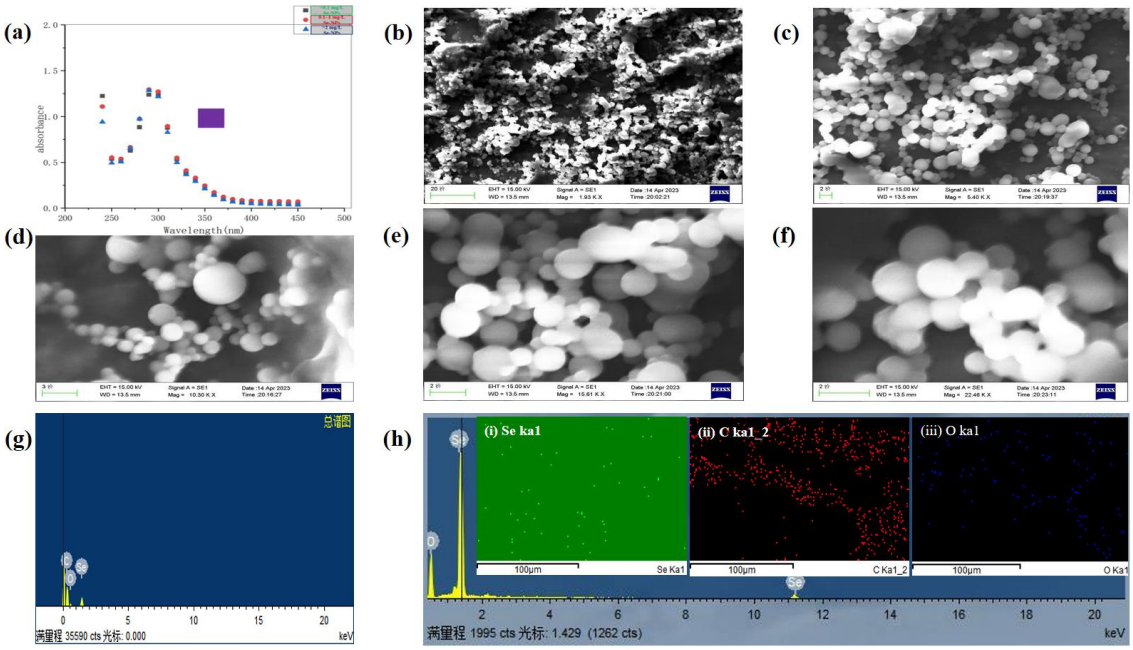


Fig. 1. Characterization of Se-NPs before and after incubation with cultured yeast strain under optimal conditions. (a) UV−Vis spectra. SEM (b) before and (c) after (d) <0.1 mg/L Se-NPs (e) 0.1–1 mg/L Se-NPs (f) >2 mg/L Se-NPs incubation yeast strain. EDS (g) before and (h) after incubation yeast strain (i) for selenium (ii) for carbon (iii) for oxygen.

3.2 Microscopic analysis of Se-NPs on morphology of yeast cells

Microscopic imaging revealed substantial morphological changes across different selenium treatments in yeast cells. In selenium-free conditions, yeast cells displayed a standard elliptical morphology with clearly visible cellular boundaries. However, some cells exhibited minor cytoplasmic granulation and slightly enlarged vacuoles, indicating basal oxidative activity. Mitochondria appeared slightly diffused but structurally intact, suggesting minimal intrinsic stress in the absence of external selenium supplementation (Fig. 2a). In low selenium concentrations (<0.1 mg/L), cells displayed slight improvements in morphology compared to the control group. Cellular boundaries were more defined, vacuoles appeared regular in size, and mitochondrial clarity improved. Cytoplasmic granulation was reduced, indicating mild selenium-induced enhancement of basal redox buffering capacity (Fig. 2b). At moderate selenium concentrations (0.1–1 mg/L), cells exhibited optimal morphology. They maintained a healthy, uniform elliptical structure with minimal cytoplasmic granules and well-defined vacuoles. Mitochondrial structure was robust, indicating enhanced energy metabolism and redox homeostasis. No indications of cellular stress or toxicity were observed at this concentration under basal conditions **(**Fig. 2c**)**. Yeast cells exposed to high selenium concentrations displayed noticeable morphological abnormalities. Vacuoles were disproportionately enlarged, mitochondria appeared fragmented, and some cells showed irregular shapes, suggesting the onset of selenium-induced toxicity. Cytoplasmic granulation increased significantly, indicative of oxidative stress caused by excess selenium **(**Fig. 2d**)**. These findings highlight the importance of selenium concentration in maintaining cellular health and homeostasis by reflecting that, low selenium concentrations (<0.1 mg/L) improved biomass production and optimal growth observed at moderate levels (0.1–1 mg/L). In contrast, high selenium concentrations (>2 mg/L) negatively impacted yeast growth as suggested in [38].

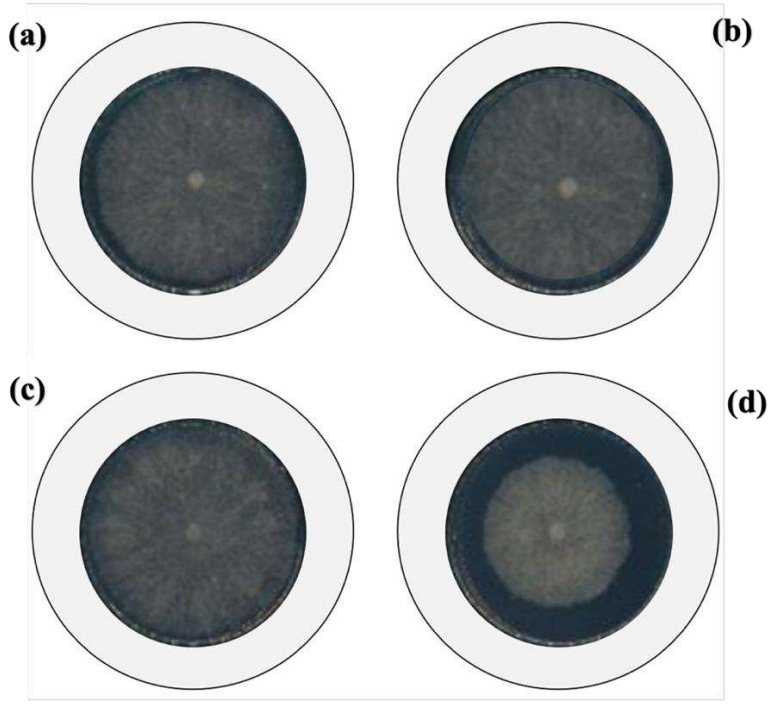


Fig. 2. Microscopic analysis of different selenium treatments on yeast cells (a) control (b) low selenium concentrations (<0.1 mg/L) (c) moderate selenium concentrations (0.1–1 mg/L) (d) high selenium concentrations (>2 mg/L).

3.3 Spectroscopic analysis of growth dynamics and proliferation of yeast cells

Culture growth analysis through A600 measurements at 0, 12, 24, 36, and 48 hours revealed a different response to varying selenium concentration under optimal growth conditions (Fig. 3a). At 0 hours, optical density (OD600) values started similarly across all selenium concentrations (~0.10), reflecting uniform initial inoculation. After 12 hours, growth was observed in all conditions such as OD600 for no selenium (0.45), <0.1 mg/L selenium concentrations (0.55), 0.1–1 mg/L selenium concentrations (0.70) and >2 mg/L selenium concentrations (0.40). After 24 hours, spectroscopic measurements revealed a baseline OD600 of 0.75, representing standard biomass production in the absence of selenium supplementation. This indicates typical cell proliferation and metabolic activity. Cultures treated with low selenium concentrations (<0.1 mg/L) exhibited a marginal increase in OD600, reaching 0.85. This slight

enhancement in biomass production suggests a subtle improvement in growth efficiency, potentially due to low-level stimulation of antioxidant systems and cellular processes. At moderate selenium concentrations (0.1–1 mg/L), yeast cells demonstrated a significant increase in biomass production, with OD600 reaching 1.12. This improvement indicates optimal growth conditions, enhancing cellular metabolic activity and redox regulation. Cultures exposed to high selenium concentrations (>2 mg/L) exhibited a reduced OD600, measured at 0.66. This decline in biomass indicates inhibited growth, likely due to the pro-oxidant effects of excessive selenium leading to cellular stress, metabolic disruption and possible toxicity. After 36 hours, growth started plateauing as nutrients were consumed. OD600 dropped slightly for no selenium (0.60) and <0.1 mg/L selenium concentrations (0.70). 0.1–1 mg/L selenium concentrations maintained a high OD600 (1.00). A sharp decline was observed for >2 mg/L selenium concentrations (0.45). After 48 hours, growth decreased due to nutrient depletion and potential accumulation of waste products. OD600 dropped for no selenium (0.50) and <0.1 mg/L selenium concentrations (0.60). 0.1–1 mg/L selenium concentrations still had the highest OD600 (0.90). OD600 declined significantly in >2 mg/L selenium concentrations (0.35), indicating severe toxicity effects. This data indicates that selenium supplementation within 0.1–1 mg/L ranges supports yeast proliferation, reflecting growth-promoting effects at these optimal. As suggested in previous reports[39] .

Cell cycle progression was assessed using a hemocytometer under different selenium treatments. The percentage of cells in G1, S and G2/M phases was determined by counting cells at each stage (Fig. 3b). In no selenium treatment, G1 phase, S phase and G2/M phase contained 60% ± 2.1, 25% ± 1.4 and 15% ± 1.5 cells respectively, exhibited normal yeast cell cycle distribution, with a majority of cells arrested in the G1 phase,

indicative of a typical proliferation cycle under standard growth conditions. In low selenium concentrations (<0.1 mg/L), G1 phase, S phase and G2/M phase contained 55% ± 2.0, 30% ± 1.3 and 15% ± 1.2 cells respectively, showed a slight reduction in the G1 phase population, with an increased percentage of cells in S phase. This indicates an improvement in DNA synthesis and cell cycle progression compared to the control. In moderate selenium concentrations (0.1–1 mg/L), G1 phase, S phase and G2/M phase contained 50% ± 2.5, 35% ± 1.5 and 15% ± 1.3 cells respectively, represented a substantial increase in S phase cells and reduction in G1 phase cells, correlating with enhanced cell proliferation and DNA replication compared to the control. So selenium within moderate ranges stimulates cell cycle progression, contributing to higher yeast growth rates. In high selenium concentrations (>2 mg/L), G1 phase, S phase and G2/M phase contained 70% ± 3.1, 20% ± 1.1 and 10% ± 1.4 cells respectively, led to a significant increase in the G1 phase population, with a marked reduction in S phase population. This indicates a delay in cell cycle progression, potentially due to oxidative stress and cellular damage impairing DNA replication and cell division. The decreased G2/M population further supports the idea that high selenium concentrations induce cytotoxic effects, limiting cellular proliferation similar results were suggested by [40].

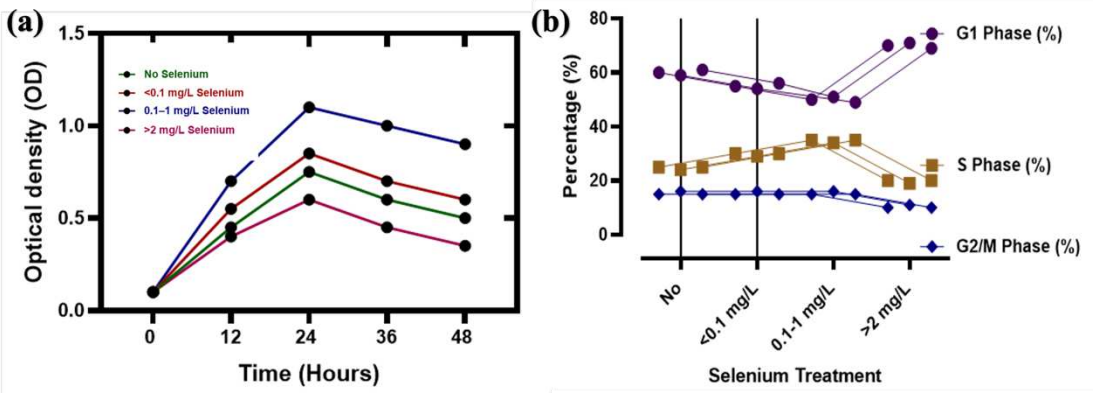


Fig. 3. Yeast cells analysis (a) spectroscopic absorbance of different selenium treatments (b) cell counts of different selenium treatments.

3.4 Effect of selenium NPs on yeast' mitochondrial, cytosolic, and nuclear GSH:GSSG under cold shock and heat shock

The impact of different selenium treatments during both normal condition and thermal stress condition on the GSH:GSSG ratio was evaluated across three cellular compartments: mitochondria, cytosol, and nucleus in yeast cells to evaluate selenium's impact on glutathione redox balance (Fig. 4).

Under no thermal stress condition (control), a balanced mitochondrial GSH:GSSG ratio (8.0) was observed, indicating normal redox homeostasis in no selenium supplementation. In low selenium (<0.1 mg/L) supplementation, a mild increase (10.0) was detected, reflecting moderate improvement in redox balance due to selenium's antioxidant role. In moderate selenium (0.1–1 mg/L) supplementation, the highest ratio (14.0) was recorded, suggesting optimal selenium-enhanced glutathione recycling and mitochondrial protection. In high selenium (>2 mg/L) supplementation, a marked decrease (11.0) indicated oxidative stress, suggesting a pro-oxidant effect. Under cold shock condition, the mitochondrial GSH:GSSG ratio moderately declined to 2.0, reflecting redox stress from metabolic slowing in no selenium supplementation. In low selenium (<0.1 mg/L) supplementation, a slight improvement (4.0) was observed, suggesting mild redox stabilization. In moderate selenium (0.1–1 mg/L) supplementation, the highest ratio (8.0) was analyzed, indicating selenium-enhanced glutathione activity for mitochondrial stress adaptation. In high selenium (>2 mg/L) supplementation, the lowest value (5.0) was evaluated, highlighting severe redox imbalance and cold stress sensitivity due to selenium toxicity. Under heat shock condition, the mitochondrial GSH:GSSG ratio dropped to 1.0, indicating heat induced oxidative stress in no selenium supplementation. In low selenium (<0.1 mg/L)

supplementation, a minor improvement (2.0) was observed, suggesting a mild protective role. In moderate selenium (0.1–1 mg/L) supplementation, a significant increase (7.0) was observed, demonstrating strong mitochondrial resilience to heat stress. In high selenium (>2 mg/L) supplementation, the lowest ratio (3.0) was recorded, indicating excessive ROS accumulation and mitochondrial dysfunction (Fig. 4a).

Under no thermal stress condition (control), a balanced cytosolic GSH:GSSG ratio (12.0) was observed, indicating normal redox homeostasis in no selenium supplementation. In low selenium (<0.1 mg/L) supplementation, a mild increase (14.0) was detected, reflecting moderate improvement in redox balance due to selenium's antioxidant role. In moderate selenium (0.1–1 mg/L) supplementation, the highest ratio (18.0) was recorded, suggesting optimal selenium-enhanced glutathione recycling. In high selenium (>2 mg/L) supplementation, a marked decrease (15.0) indicated oxidative stress, implying an imbalance in redox homeostasis. Under cold shock condition, the cytosolic GSH:GSSG ratio moderately declined to 5.0, reflecting cold-induced redox stress in no selenium supplementation. In low selenium (<0.1 mg/L) supplementation, a slight improvement (7.0) was observed, suggesting slight selenium-mediated protection. In moderate selenium (0.1–1 mg/L) supplementation, the highest ratio (12.0) was determined, indicating enhanced antioxidant capacity and improved redox stability. In high selenium (>2 mg/L) supplementation, the lowest value (8.0) highlighted severe cytosolic redox imbalance, indicating pro-oxidant effects at toxic selenium doses. Under heat shock condition, the cytosolic GSH:GSSG ratio dropped to 3.0, indicating heat induced oxidative stress in no selenium supplementation. In low selenium (<0.1 mg/L) supplementation, a modest improvement (5.0) was observed, suggesting a mild protective role. In moderate selenium (0.1–1 mg/L) supplementation, the highest ratio (11.0) was recorded, indicating strong cytosolic redox stabilization and

stress adaptation. In high selenium (>2 mg/L) supplementation, the lowest ratio (6.0) was recorded, indicating excessive ROS accumulation (Fig. 4b).

Under no thermal stress condition (control), a balanced nuclear GSH:GSSG ratio (10.0) was observed, indicating stable redox homeostasis in no selenium supplementation. In low selenium (<0.1 mg/L) supplementation, a mild increase (12.0) was detected, reflecting slight enhancement of nuclear antioxidant defense. In moderate selenium (0.1–1 mg/L) supplementation, the highest ratio (16.0) was recorded, suggesting optimal selenium-mediated nuclear redox stabilization. In high selenium (>2 mg/L) supplementation, a significant decline (13.0) was observed, suggesting redox imbalance and potential oxidative damage. Under cold shock condition, the nuclear GSH:GSSG ratio moderately declined to 4.0, reflecting cold-induced nuclear oxidative stress in no selenium supplementation. In low selenium (<0.1 mg/L) supplementation, a slight improvement (6.0) was imparted, suggesting mild nuclear redox stabilization. In moderate selenium (0.1–1 mg/L) supplementation, the highest ratio (10.0) was indicated, reflecting effective nuclear antioxidant activity and DNA protection. In high selenium (>2 mg/L) supplementation, a decrease (7.0) indicated nuclear oxidative stress, imparting pro-oxidant effects of excessive selenium. Under heat shock condition, the nuclear GSH:GSSG ratio dropped to 2.5, indicating oxidative stress-induced redox imbalance in no selenium supplementation. In low selenium (<0.1 mg/L) supplementation, a modest increase (4.0) was observed, suggesting slight nuclear protection against heat-induced oxidative stress. In moderate selenium (0.1–1 mg/L) supplementation, the highest ratio (9.0) was recorded, demonstrating strong nuclear redox regulation and stress adaptation. In high selenium (>2 mg/L) supplementation, the lowest ratio (5.0) suggested increased oxidative stress, affecting nuclear integrity due to excess ROS accumulation (Fig. 4c).

These findings highlighted the concentration-dependent role of selenium in mitochondrial redox homeostasis, cytosolic redox homeostasis and nuclear redox regulation, emphasizing its antioxidant benefits at optimal doses (0.1–1 mg/L) and its oxidative potential at excessive concentrations (>2 mg/L) under thermal stress conditions suggested [41].

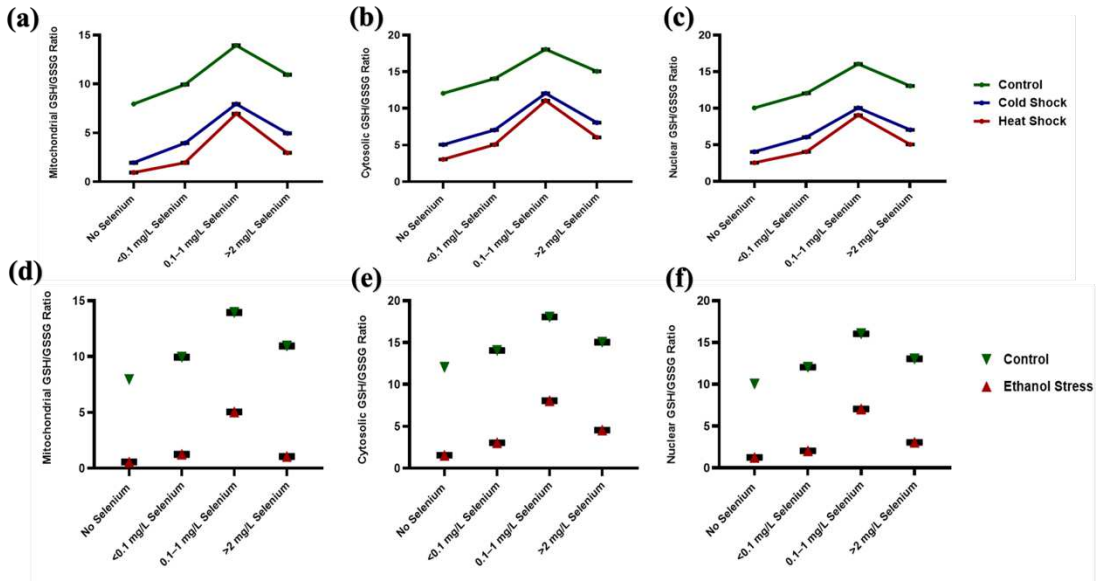


Fig. 4. Effect of different selenium treatments on yeast' (a) mitochondrial (b) cytosolic (c) nuclear GSH:GSSG ratio under control, cold shock and heat shock (d) Ethanol stress and mitochondrial (e) Ethanol induced cytosolic (f) nuclear GSH:GSSG ratio under both control and ethanol-induced stress

3.5 Effect of selenium NPs on yeast' mitochondrial, cytosolic, and nuclear GSH:GSSG ratio under ethanol-induced stress

The impact of different selenium treatments during both normal condition and ethanol-induced stress condition on the GSH:GSSG ratio was evaluated across three cellular compartments: mitochondria, cytosol, and nucleus in yeast cells to evaluate selenium's impact on glutathione redox balance (Fig. 4d).

Under no ethanol stress condition (control), a balanced mitochondrial GSH:GSSG ratio (8.0) was observed, indicating stable redox homeostasis in no selenium

supplementation. In low selenium (<0.1 mg/L) supplementation, a slight increase (10.0) was observed, indicating minor enhancement of mitochondrial antioxidant defenses. In moderate selenium (0.1–1 mg/L) supplementation, the highest ratio (14.0) was recorded, suggesting an optimal redox state and enhanced mitochondrial protection. In high selenium (>2 mg/L) supplementation, a significant decline (11.0) suggested redox imbalance, potentially due to selenium-induced ROS generation. Under ethanol-induced stress condition, the mitochondrial GSH:GSSG ratio dropped to 0.5, indicating oxidative stress and mitochondrial dysfunction in no selenium supplementation. In low selenium (<0.1 mg/L) supplementation, a minor increase (1.2) was observed, suggesting slight mitigation of ethanol-induced oxidative stress. In moderate selenium (0.1–1 mg/L) supplementation, the highest ratio (5.0) was recorded, highlighting strong mitochondrial antioxidant activity and resistance to ethanol toxicity. In high selenium (>2 mg/L) supplementation, the lowest ratio (1.0) was observed, indicating excessive oxidative stress, mitochondrial damage, and potential apoptosis induction (Fig. 4d).

Under no ethanol stress condition (control), a balanced cytosolic GSH:GSSG ratio (12.0) was observed, indicating well-maintained redox homeostasis in no selenium supplementation. In low selenium (<0.1 mg/L) supplementation, a mild increase (14.0) was detected, reflecting a mild enhancement of antioxidant capacity. In moderate selenium (0.1–1 mg/L) supplementation, the highest ratio (18.0) was recorded, demonstrating optimal redox homeostasis and enhanced glutathione recycling efficiency. In high selenium (>2 mg/L) supplementation, a significant reduction (15.0) was observed, indicating a shift towards oxidative stress, likely due to excessive selenium-induced ROS accumulation. Under ethanol-induced stress condition, the cytosolic GSH:GSSG ratio dropped to 1.5, indicating oxidative stress and depletion of reduced glutathione in no selenium supplementation. In low selenium (<0.1 mg/L)

supplementation, a slight increase (3.0) was noted, suggesting mild protection against ethanol-induced redox imbalance. In moderate selenium (0.1–1 mg/L) supplementation, the highest ratio (8.0) was observed, highlighting selenium's protective role in maintaining cytosolic redox balance. In high selenium (>2 mg/L) supplementation, a severe decline (4.5) was recorded, suggesting increased oxidative stress and potential cytotoxicity (Fig. 4e).

Under no ethanol stress condition (control), a balanced nuclear GSH:GSSG ratio (10.0) was observed, maintaining an optimal redox environment for nuclear function in no selenium supplementation. In low selenium (<0.1 mg/L) supplementation, a slight increase (12.0) was observed, indicating mild selenium-induced enhancement of nuclear redox potential. In moderate selenium (0.1–1 mg/L) supplementation, the highest ratio (16.0) suggested improved nuclear antioxidant defense, facilitating redox-sensitive transcriptional regulation. In high selenium (>2 mg/L) supplementation, a marked reduction (13.0) indicated oxidative stress, potentially impairing nuclear redox homeostasis and DNA repair processes. Under ethanol-induced stress condition, the nuclear GSH:GSSG ratio dropped to 1.2, reflecting ethanol-induced nuclear oxidative stress in no selenium supplementation. In low selenium (<0.1 mg/L) supplementation, a moderate increase (2.0) was observed, suggesting limited protective effects against ethanol-induced nuclear redox imbalance. In moderate selenium (0.1–1 mg/L) supplementation, the highest ratio (7.0) indicated an enhanced nuclear antioxidant response, mitigating ethanol-induced oxidative damage. In high selenium (>2 mg/L) supplementation, a severe decline (3.0) suggested excessive oxidative stress, potentially disrupting nuclear integrity and transcriptional regulation (Fig. 4f).

These results highlighted the dose-dependent role of selenium in mitochondrial redox homeostasis, cytosolic redox balance and nuclear redox stability, with optimal

supplementation (0.1–1 mg/L) enhancing stress resilience and excessive doses (>2 mg/L) leading to oxidative damage under ethanol stress conditions suggested[42].

3.6 Effect of selenium NPs on yeast' mitochondrial, cytosolic, and nuclear GSH:GSSG ratio under H_2O_2-induced stress

The impact of different selenium treatments during both normal condition and H_2O_2-induced stress condition on the GSH:GSSG ratio was evaluated across three cellular compartments: mitochondria, cytosol, and nucleus in yeast cells to evaluate selenium's impact on glutathione redox balance (Fig. 5).

Under no H_2O_2 stress condition (control), a balanced mitochondrial GSH:GSSG ratio (8.0) was observed, indicating stable redox homeostasis in no selenium supplementation. In low selenium (<0.1 mg/L) supplementation, a slight increase (10.0) was observed, indicating minor enhancement of mitochondrial antioxidant defenses. In moderate selenium (0.1–1 mg/L) supplementation, the highest ratio (14.0) was recorded, suggesting an optimal redox state and enhanced glutathione recycling. In high selenium (>2 mg/L) supplementation, a significant decline (11.0) suggested redox imbalance, potentially due to selenium-induced ROS generation. Under H_2O_2-induced stress condition, the mitochondrial GSH:GSSG ratio dropped to 0.7, indicating oxidative stress and glutathione depletion in no selenium supplementation. In low selenium (<0.1 mg/L) supplementation, a minor increase (1.5) was observed, suggesting slight mitigation of H_2O_2-induced oxidative stress. In moderate selenium (0.1–1 mg/L) supplementation, the highest ratio (5.0) was recorded, highlighting strong mitochondrial antioxidant activity and resistance to H_2O_2 toxicity. In high selenium (>2 mg/L) supplementation, the lowest ratio (1.2) was observed, indicating excessive oxidative stress and mitochondrial damage (Fig. 5a).

Under no H_2O_2 stress condition (control), a balanced cytosolic GSH:GSSG ratio (12.0) was observed, indicating well-maintained redox homeostasis in no selenium supplementation. In low selenium (<0.1 mg/L) supplementation, a mild increase (14.0) was detected, reflecting a mild enhancement of antioxidant capacity. In moderate selenium (0.1–1 mg/L) supplementation, the highest ratio (18.0) was recorded, demonstrating optimal redox homeostasis and enhanced glutathione recycling efficiency. In high selenium (>2 mg/L) supplementation, a significant reduction (15.0) was observed, indicating a shift towards oxidative stress, likely due to excessive selenium-induced ROS accumulation. Under H_2O_2-induced stress condition, the cytosolic GSH:GSSG ratio dropped to 2.0, indicating oxidative stress and depletion of reduced glutathione in no selenium supplementation. In low selenium (<0.1 mg/L) supplementation, a slight increase (3.0) was noted, suggesting mild protection against H_2O_2-induced redox imbalance. In moderate selenium (0.1–1 mg/L) supplementation, the highest ratio (10.0) was observed, highlighting selenium's protective role in maintaining cytosolic redox balance. In high selenium (>2 mg/L) supplementation, a severe decline (5.0) was recorded, suggesting increased oxidative stress and potential cytotoxicity due to glutathione depletion (Fig. 5b).

Under no H_2O_2 stress condition (control), a balanced nuclear GSH:GSSG ratio (10.0) was observed, maintaining an optimal redox environment for nuclear function in no selenium supplementation. In low selenium (<0.1 mg/L) supplementation, a slight increase (12.0) was observed, indicating mild selenium-induced enhancement of nuclear glutathione. In moderate selenium (0.1–1 mg/L) supplementation, the highest ratio (16.0) suggested improved nuclear antioxidant defense, facilitating redox-sensitive transcriptional regulation and DNA repair. In high selenium (>2 mg/L) supplementation, a marked reduction (13.0) indicated oxidative stress, potentially

impairing nuclear redox homeostasis and DNA repair processes due to nuclear glutathione depletion. Under H_2O_2-induced stress condition, the nuclear GSH:GSSG ratio dropped to 1.5, reflecting H_2O_2-induced nuclear oxidative stress in no selenium supplementation. In low selenium (<0.1 mg/L) supplementation, a moderate increase (2.5) was observed, suggesting limited protective effects against H_2O_2-induced nuclear redox imbalance. In moderate selenium (0.1–1 mg/L) supplementation, the highest ratio (8.0) indicated an enhanced nuclear antioxidant response, mitigating H_2O_2-induced oxidative DNA damage. In high selenium (>2 mg/L) supplementation, a severe decline (3.5) suggested excessive oxidative stress, potentially disrupting nuclear integrity and transcriptional regulation due to impaired glutathione recycling (Fig. 5c).

These findings emphasized the dose-dependent role of selenium in mitochondrial redox regulation, cytosolic redox balance and nuclear antioxidant defenses, demonstrating its protective effect at optimal levels (0.1–1 mg/L) and its oxidative potential at excessive concentrations (>2 mg/L) under H_2O_2 stress conditions suggested[39].

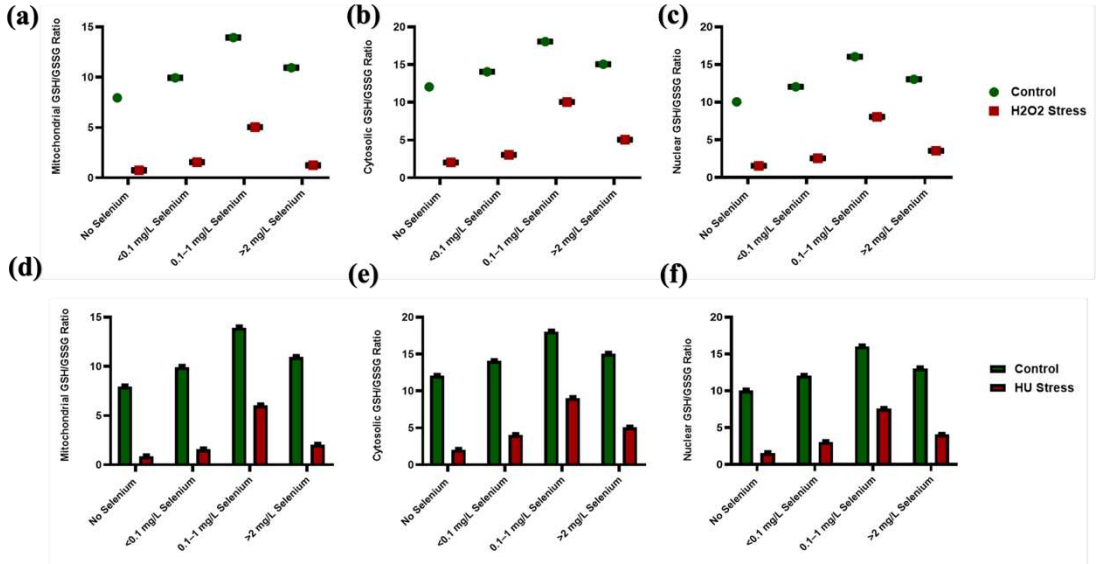


Fig. 5. Effect of different selenium treatments on yeast' (a) mitochondrial (b) cytosolic (c) nuclear GSH:GSSG ratio under both control and H_2O_2-induced stress. HU-induced

stress (d) mitochondrial (e) cytosolic (f) nuclear GSH:GSSG ratio under both control and HU-induced stress.

3.7 Effect of selenium NPs on yeast' mitochondrial, cytosolic, and nuclear GSH:GSSG ratio under HU-induced stress

The impact of different selenium treatments during both normal condition and HU-induced stress condition on the GSH:GSSG ratio was evaluated across three cellular compartments: mitochondria, cytosol, and nucleus in yeast cells to evaluate selenium's impact on glutathione redox balance (Fig. 5d).

Under no HU stress condition (control), a balanced mitochondrial GSH:GSSG ratio (8.0) was observed, indicating stable redox homeostasis in no selenium supplementation. In low selenium (<0.1 mg/L) supplementation, a slight increase (10.0) was observed, indicating minor enhancement of mitochondrial antioxidant defenses. In moderate selenium (0.1–1 mg/L) supplementation, the highest ratio (14.0) was recorded, suggesting an optimal redox state and enhanced glutathione recycling. In high selenium (>2 mg/L) supplementation, a significant decline (11.0) suggested redox imbalance, potentially due to selenium-induced ROS generation. Under HU-induced stress condition, the mitochondrial GSH:GSSG ratio dropped to 0.8, indicating oxidative stress and glutathione depletion in no selenium supplementation. In low selenium (<0.1 mg/L) supplementation, a minor increase (1.5) was observed, suggesting slight mitigation of HU-induced oxidative stress. In moderate selenium (0.1–1 mg/L) supplementation, the highest ratio (6.0) was recorded, highlighting strong mitochondrial antioxidant activity and resistance to HU toxicity. In high selenium (>2 mg/L) supplementation, the lowest ratio (2.0) was observed, indicating excessive oxidative stress and mitochondrial damage (Fig. 5d).

Under no HU stress condition (control), a balanced cytosolic GSH:GSSG ratio (12.0) was observed, indicating well-maintained redox homeostasis in no selenium supplementation. In low selenium (<0.1 mg/L) supplementation, a mild increase (14.0) was detected, reflecting a mild enhancement of antioxidant capacity. In moderate selenium (0.1–1 mg/L) supplementation, the highest ratio (18.0) was recorded, demonstrating optimal redox homeostasis and enhanced glutathione recycling efficiency. In high selenium (>2 mg/L) supplementation, a significant reduction (15.0) was observed, indicating a shift towards oxidative stress, likely due to excessive selenium-induced ROS accumulation. Under HU-induced stress condition, the cytosolic GSH:GSSG ratio dropped to 2.0, indicating oxidative stress and depletion of reduced glutathione in no selenium supplementation. In low selenium (<0.1 mg/L) supplementation, a slight increase (4.0) was noted, suggesting mild protection against HU-induced redox imbalance. In moderate selenium (0.1–1 mg/L) supplementation, the highest ratio (9.0) was observed, highlighting selenium's protective role in maintaining cytosolic redox balance. In high selenium (>2 mg/L) supplementation, a severe decline (5.0) was recorded, suggesting increased oxidative stress and potential cytotoxicity due to glutathione depletion (Fig. 5e).

Under no HU stress condition (control), a balanced nuclear GSH:GSSG ratio (10.0) was observed, maintaining an optimal redox environment for nuclear function in no selenium supplementation. In low selenium (<0.1 mg/L) supplementation, a slight increase (12.0) was observed, indicating mild selenium-induced enhancement of nuclear glutathione. In moderate selenium (0.1–1 mg/L) supplementation, the highest ratio (16.0) suggested improved nuclear antioxidant defense, facilitating redox-sensitive transcriptional regulation and DNA repair. In high selenium (>2 mg/L) supplementation, a marked reduction (13.0) indicated oxidative stress, potentially

impairing nuclear redox homeostasis and DNA repair processes due to nuclear glutathione depletion. Under HU-induced stress condition, the nuclear GSH:GSSG ratio dropped to 1.5, reflecting HU-induced nuclear oxidative stress in no selenium supplementation. In low selenium (<0.1 mg/L) supplementation, a moderate increase (3.0) was observed, suggesting limited protective effects against HU-induced nuclear redox imbalance. In moderate selenium (0.1–1 mg/L) supplementation, the highest ratio (7.5) indicated an enhanced nuclear antioxidant response, mitigating HU-induced oxidative DNA damage. In high selenium (>2 mg/L) supplementation, a severe decline (4.0) suggested excessive oxidative stress, potentially disrupting nuclear integrity and transcriptional regulation due to impaired glutathione recycling (Fig. 5f).

These findings emphasized the dose-dependent role of selenium in mitochondrial redox regulation, cytosolic redox balance and nuclear antioxidant defenses, demonstrating its protective effect at optimal levels (0.1–1 mg/L) and its oxidative potential at excessive concentrations (>2 mg/L) under HU stress conditions suggested [43].

Thermal stress effects on protein stability and cellular function[44]. Ethanol exposure simulates the impact of fermentation-related stress commonly encountered in industrial processes[45, 46] . Oxidative stress from H_2O_2 provides insight into the role of selenium in combating ROS [47], while HU-induced replication stress probes its influence on DNA replication fidelity[48] under challenging conditions[49]. These stressors offer a comprehensive framework to evaluate exogenous selenium's protective[50] and potentially toxic [51] effects. Selenium imbalance disrupts critical biomolecules such as lipids [52], proteins [53], and DNA[54], triggering cellular damage and apoptosis[55]. Additionally, the incorporation of excess selenium into nonspecific proteins can lead to selenoprotein misfolding and impaired functionality, exacerbating cellular toxicity[56, 57]. In conclusion, this study reveals the complex dynamics

between Se-NPs, yeast physiology and immunity, and stressors for addressing dose-dependent selenium beneficial and toxic impacts on growth and GSH:GSSG cycle in *Saccharomyces cerevisiae* exposed to external stress conditions (Fig. 6ab). Depending on its concentration, selenium can have both positive and negative effects.

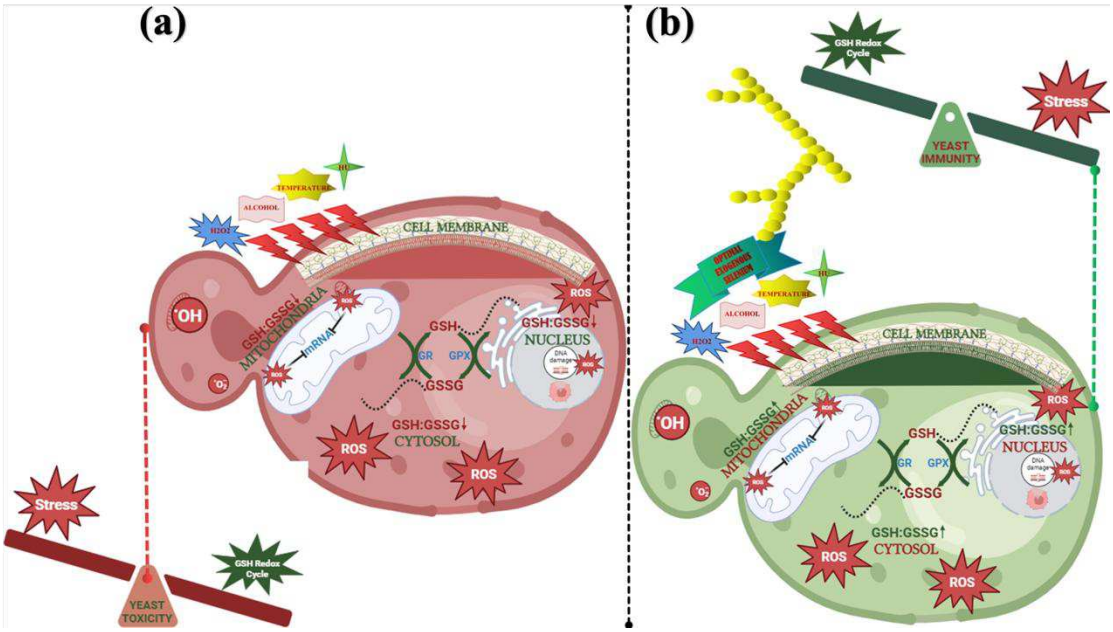


Fig. 6. Growth and glutathione redox cycle in *Saccharomyces cerevisiae* under (a) selenium free condition (b) selenium optimal dose condition.

4. Conclusion

In this paper, we developed a green synthesis method that uses *C.sativus* as an efficient reducing and stabilizing agent to synthesize Se-NPs in a simple, economical, and environmental friendly manner without the use of any toxic or hazardous materials. Through UV-Vis, SEM, and EDS characterization of Se-NPs before and after treated with yeast culture, it was verified that the Se-NPs had been green synthesized. Se-NPs displayed a 300 nm-wavelength SPR band. Further, analysis showed that green synthesized Se-NPs have an irregular, spherical shape and are 100 nm in size.

Additionally, Se is present at a strong intensity than that of carbon and oxygen. The study's findings showed that Se-NPs supplementation had dose-dependent effects on the growth in *Saccharomyces cerevisiae*. Changes in cell morphology as seen by microscopy, biomass production as determined by spectroscopic absorbance at A 600, and cell proliferation as determined by cell counts are among the important parameters which examined. These parameters are interconnected because spectroscopic absorbance acts as a proxy for overall biomass and metabolic activity, and morphological changes frequently correspond with variations in cell viability and proliferation rates. By measuring the GSH:GSSG ratio in the mitochondria, cytosol, and nucleus of yeast exposed to a variety of external stressors, including thermal, ethanol, hydrogen peroxide (H_2O_2), and hydroxyurea (HU) stressors, this study has also investigated the dose-dependent dual nature of selenium. By improving antioxidant defense systems and preserving redox homeostasis, optimal Se-NPs supplementation (0.1–1 mg/L) reinforced the yeast's resistance to these stresses, as evidenced of improving GSH:GSSG ratios across cellular compartments. Excessive Se-NPs supplementation (>2 mg/L) induced cellular toxicity and oxidative stress. With implications for industrial fermentation processes, oxidative stress mitigation and cellular redox regulations, the significance of the optimal dose of Se-NPs supplementation is highlighted in biotechnological applications and stress managements. For potential applications in metabolic engineering and cellular defense strategies, more research is required to understand the mechanistic pathways of selenium in yeast.

Funding declaration:

There is no funding to support this studies

Declaration

Ethics approval

This study was not involving any human participants or experimental animals, therefore, there is no need of any ethical approval for this work.

Author Contribution declaration

H. G: experimentation, data collection, investigation, manuscript writing,

A. G: Data interpretation, visualization, data collection,

I. A: visualization, software, data collection,

N. F: xperimentation, data collection, methodology

M. Z. N: Software, investigation, experimentation

M.S.S: visualization, software, data collection,

D.B: Data interpretation, visualization, data collection,

X. H: Supervision, conceputilization, management of manuscript

M. H: Supervision, conceputilization, Darft writing,

Competing Interest

All the authors in the manuscript declare for no competing interests.

Consent to Participate

Not applicable.

Consent to Publish

Not applicable.

Availability of Data and Materials

The data supporting the findings of this study are available from the corresponding author upon reasonable request.

References

1. Ahmad, W., Shams, S., Ahmad, A., Wei, Y., Yuan, Q., Khan, A. U., … Iqbal, M. (2020). Synthesis of selenium–silver nanostructures with enhanced antibacterial, photocatalytic and antioxidant activities. *Applied Nanoscience (Switzerland)*. https://doi.org/10.1007/s13204-019-01213-z
2. Wu, Z., Ren, Y., Liang, Y., Huang, L., Yang, Y., Zafar, A., … Shu, X. (2021). Synthesis, Characterization, Immune Regulation, and Antioxidative Assessment of Yeast-Derived Selenium Nanoparticles in Cyclophosphamide-Induced Rats. *ACS Omega*, *6*(38), 24585–24594. https://doi.org/10.1021/acsomega.1c03205

3. Ahmed, M. M., Mukheed, M., Tariq, T., Hasan, M., Shaaban, M., Mustafa, G., & Hatami, M. (2025). Physio-biochemical insights into Arsenic stress mitigation regulated by Selenium nanoparticles in Gossypium hirsutum L. *BMC Plant Biology*, *25*(1). https://doi.org/10.1186/s12870-025-06514-w
4. Chen, F., Aqeel, M., Khalid, N., Irshad, M. K., Farhat, F., Nazir, A., … Noman, A. (2023). Glutathione treatment suppresses the adverse effects of microplastics in rice. *Chemosphere*, *322*. https://doi.org/10.1016/j.chemosphere.2023.138079
5. Habig, W. H., Pabst, M. J., & Jakoby, W. B. (1974). Glutathione S transferases. The first enzymatic step in mercapturic acid formation. *Journal of Biological Chemistry*, *249*(22).
6. Hasanuzzaman, M., Borhannuddin Bhuyan, M. H. M., Anee, T. I., Parvin, K., Nahar, K., Al Mahmud, J., & Fujita, M. (2019). Regulation of ascorbate-glutathione pathway in mitigating oxidative damage in plants under abiotic stress. *Antioxidants*. https://doi.org/10.3390/antiox8090384
7. Labunskyy, V. M., Hatfield, D. L., & Gladyshev, V. N. (2014). Selenoproteins: Molecular pathways and physiological roles. *Physiological Reviews*. https://doi.org/10.1152/physrev.00039.2013
8. Truong, V. L., Jun, M., & Jeong, W. S. (2018). Role of resveratrol in regulation of cellular defense systems against oxidative stress. *BioFactors*. https://doi.org/10.1002/biof.1399
9. Lu, S. C. (2013). Glutathione synthesis. *Biochimica et Biophysica Acta - General Subjects*. https://doi.org/10.1016/j.bbagen.2012.09.008
10. Grant, C. M. (2001). Role of the glutathione/glutaredoxin and thioredoxin systems in yeast growth and response to stress conditions. *Molecular Microbiology*. https://doi.org/10.1046/j.1365-2958.2001.02283.x
11. Avery, S. V. (2001). Metal toxicity in yeasts and the role of oxidative stress. *Advances in Applied Microbiology*. https://doi.org/10.1016/S0065-2164(01)49011-3
12. Jamieson, D. J. (1998). Oxidative stress responses of the yeast Saccharomyces cerevisiae. *Yeast*. https://doi.org/10.1002/(SICI)1097-0061(199812)14:16<1511::AID-YEA356>3.0.CO;2-S
13. Cabiscol, E., Piulats, E., Echave, P., Herrero, E., & Ros, J. (2000). Oxidative stress promotes specific protein damage in Saccharomyces cerevisiae. *Journal of Biological Chemistry*, *275*(35). https://doi.org/10.1016/s0021-9258(19)61523-1
14. Moradas-Ferreira, P., & Costa, V. (2000). Adaptive response of the yeast Saccharomyces cerevisiae to reactive oxygen species: Defences, damage and death. *Redox Report*. https://doi.org/10.1179/135100000101535816
15. Dawood, M. A. O., Zommara, M., Eweedah, N. M., Helal, A. I., & Aboel-Darag, M. A. (2020). The potential role of nano-selenium and vitamin C on the performances of Nile tilapia (Oreochromis niloticus). *Environmental Science and Pollution Research*. https://doi.org/10.1007/s11356-020-07651-5
16. Gangadoo, S., Dinev, I., Willson, N. L., Moore, R. J., Chapman, J., & Stanley, D. (2020). Nanoparticles of selenium as high bioavailable and non-toxic supplement alternatives for broiler chickens. *Environmental Science and Pollution Research*. https://doi.org/10.1007/s11356-020-07962-7
17. Bhattacharjee, A., Basu, A., & Bhattacharya, S. (2019). Selenium nanoparticles are less toxic than inorganic and organic selenium to mice in vivo. *Nucleus (India)*. https://doi.org/10.1007/s13237-019-00303-1
18. Hasan, M., Rafique, S., Zafar, A., Loomba, S., Khan, R., Hassan, S. G., … Mahmood, N. (2020). Physiological and anti-oxidative response of biologically and chemically synthesized iron oxide: Zea mays a case study. *Heliyon*. https://doi.org/10.1016/j.heliyon.2020.e04595
19. Wang, H., Zhang, J., & Yu, H. (2007). Elemental selenium at nano size possesses lower toxicity without compromising the fundamental effect on selenoenzymes: Comparison with selenomethionine in mice. *Free Radical Biology and Medicine*. https://doi.org/10.1016/j.freeradbiomed.2007.02.013
20. Mary Jacob, J., Balakrishnan, R. M., & Kumar, U. B. (2014). Biosynthesis of lead selenide quantum rods in marine Aspergillus terreus. *Materials Letters*, *124*. https://doi.org/10.1016/j.matlet.2014.03.106
21. Hasan, M., Zafar, A., Jabbar, M., Tariq, T., Manzoor, Y., Ahmed, M. M., … Mahmood, N. (2022). Trident Nano-Indexing the Proteomics Table: Next-Version Clustering of Iron Carbide NPs and Protein Corona. *Molecules*, *27*(18). https://doi.org/10.3390/molecules27185754

22. Zafar, A., Jabbar, M., Manzoor, Y., Gulzar, H., Hassan, S. G., Nazir, M. A., … Hasan, M. (2020). Quantifying Serum Derived Differential Expressed and Low Molecular Weight Protein in Breast Cancer patients. *Protein & Peptide Letters*. https://doi.org/10.2174/0929866527666200110155609
23. Qasim, S., Zafar, A., Saif, M. S., Ali, Z., Nazar, M., Waqas, M., … Hasan, M. (2020). Green synthesis of iron oxide nanorods using Withania coagulans extract improved photocatalytic degradation and antimicrobial activity. *Journal of Photochemistry and Photobiology B: Biology*. https://doi.org/10.1016/j.jphotobiol.2020.111784
24. Hasan, M., Yang, W., Ju, Y., Chu, X., Wang, Y., Deng, Y., … Hou, Y. (2017). Biocompatibility of iron carbide and detection of metals ions signaling proteomic analysis via HPLC/ESI-Orbitrap. *Nano Research*. https://doi.org/10.1007/s12274-016-1375-4
25. Hasan, M., Gulzar, H., Zafar, A., ul Haq, A., Mustafa, G., Tariq, T., … Mahmood, N. (2021). Multiplexing surface anchored functionalized iron carbide nanoparticle: A low molecular weight proteome responsive nano-tracer. *Colloids and Surfaces B: Biointerfaces*. https://doi.org/10.1016/j.colsurfb.2021.111746
26. Sun, S., Batool, S., Saba, I., Ahmed, I., Ahmad, S., Tariq, T., … Hasan, M. (2024). Biological entities of green factories for nano-grafting zinc oxide: a comparative antibacterial mechanism. *New Journal of Chemistry*. https://doi.org/10.1039/d4nj04149f
27. Tariq, T., Ahmed, I., Ahmed, M. M., Ahmad, S., Batool, R., Tauheed, S., … Hasan, M. (2025). Synthetic, biological and physiological identity of green cobalt oxide nanosponges engineered for multidrug-resistant pathogenic bacteria. *New Journal of Chemistry*. https://doi.org/10.1039/D5NJ00815H
28. Iqbal, M. F., Irshad, I., Ahmed, I., Ahmad, S., Uzair, M., Kausar, R., … Mustafa, G. (2025). Comparative study of the ability of green synthesized Se-NPs and CTS-NPs to overcome drought stress in Oryza sativa L. for regenerative nanoengineering in agriculture. *New Journal of Chemistry*. https://doi.org/10.1039/d4nj04880f
29. Kuzovlev, A. S., Volkova, D. A., Parfenova, I. V., Kulakov, I. V., Shkirdova, A. O., Zamilatskov, I. A., … Vasilchenko, A. S. (2020). Copper(i) halide and palladium(ii) chloride complexes of 4-thioxo[1,3,5]oxadiazocines: Synthesis, structure and antibacterial activity. *New Journal of Chemistry*. https://doi.org/10.1039/c9nj05958j
30. Xiao, Y., Feng, G., Mustafa, G., & Hasan, M. (2025). Improved electrocatalytic performance of TiS2 by nanohybrid with MoC nanosheets towards overall water-splitting for green hydrogen. *Fuel*, *393*. https://doi.org/10.1016/j.fuel.2025.134993
31. Zafar, S., Farooq, A., Batool, S., Tariq, T., Hasan, M., & Mustafa, G. (2024). Green synthesis of iron oxide nanoparticles for mitigation of chromium stress and anti-oxidative potential in Triticum aestivum. *Hybrid Advances*, *5*. https://doi.org/10.1016/j.hybadv.2024.100156
32. Vats, M., Bhardwaj, S., & Chhabra, A. (2020). Green Synthesis of Copper Oxide Nanoparticles using Cucumis Sativus (Cucumber) Extracts and their Bio-Physical and Biochemical Characterization for Cosmetic and Dermatologic Applications. *Endocrine, Metabolic & Immune Disorders - Drug Targets*, *21*(4). https://doi.org/10.2174/1871530320666200705212107
33. Nie, X., Zhu, Z., Lu, H., Xue, M., Tan, Z., Zhou, J., … Zhang, D. (2023). Assembly of selenium nanoparticles by protein coronas composed of yeast protease A. *Process Biochemistry*, *129*. https://doi.org/10.1016/j.procbio.2023.03.025
34. Manzoor, Y., Hasan, M., Zafar, A., Dilshad, M., Ahmed, M. M., Tariq, T., … Shu, X. (2022). Incubating Green Synthesized Iron Oxide Nanorods for Proteomics-Derived Motif Exploration: A Fusion to Deep Learning Oncogenesis. *ACS Omega*. https://doi.org/10.1021/acsomega.2c05948
35. Rieder, S. E., & Emr, S. D. (2000). Overview of Subcellular Fractionation Procedures for the Yeast Saccharomyces cerevisiae . *Current Protocols in Cell Biology*, *7*(1). https://doi.org/10.1002/0471143030.cb0307s07
36. Faramarzi, S., Anzabi, Y., & Jafarizadeh-Malmiri, H. (2020). Nanobiotechnology approach in intracellular selenium nanoparticle synthesis using Saccharomyces cerevisiae—fabrication and characterization. *Archives of Microbiology*. https://doi.org/10.1007/s00203-020-01831-0
37. Jiménez-Lamana, J., Abad-Álvaro, I., Bierla, K., Laborda, F., Szpunar, J., & Lobinski, R. (2018). Detection and characterization of biogenic selenium nanoparticles in selenium-rich yeast by single particle ICPMS. *Journal of Analytical Atomic Spectrometry*, *33*(3). https://doi.org/10.1039/c7ja00378a

38. Kieliszek, M., Błażejak, S., Bzducha-Wróbel, A., & Kot, A. M. (2019). Effect of selenium on growth and antioxidative system of yeast cells. *Molecular Biology Reports*, *46*(2). https://doi.org/10.1007/s11033-019-04630-z
39. Kaur, T., & Bansal, M. P. (2006). Selenium enrichment and anti-oxidant status in baker's yeast, Saccharomyces cerevisiae at different sodium selenite concentrations. *Nutricion Hospitalaria*, *21*(6).
40. Asghari-Paskiabi, F., Imani, M., Eybpoosh, S., Rafii-Tabar, H., & Razzaghi-Abyaneh, M. (2020). Population Kinetics and Mechanistic Aspects of Saccharomyces cerevisiae Growth in Relation to Selenium Sulfide Nanoparticle Synthesis. *Frontiers in Microbiology*, *11*. https://doi.org/10.3389/fmicb.2020.01019
41. Kieliszek, M., Bierla, K., Jiménez-Lamana, J., Kot, A. M., Alcántara-Durán, J., Piwowarek, K., … Szpunar, J. (2020). Metabolic response of the yeast candida utilis during enrichment in Selenium. *International Journal of Molecular Sciences*, *21*(15). https://doi.org/10.3390/ijms21155287
42. Herrero, E., & Wellinger, R. E. (2015). Yeast as a model system to study metabolic impact of selenium compounds. *Microbial Cell*. https://doi.org/10.15698/mic2015.05.200
43. Mapelli, V., Hillestrøm, P. R., Patil, K., Larsen, E. H., & Olsson, L. (2012). The interplay between sulphur and selenium metabolism influences the intracellular redox balance in Saccharomyces cerevisiae. *FEMS Yeast Research*, *12*(1). https://doi.org/10.1111/j.1567-1364.2011.00757.x
44. Leuenberger, P., Ganscha, S., Kahraman, A., Cappelletti, V., Boersema, P. J., Von Mering, C., … Picotti, P. (2017). Cell-wide analysis of protein thermal unfolding reveals determinants of thermostability. *Science*, *355*(6327). https://doi.org/10.1126/science.aai7825
45. Stanley, D., Bandara, A., Fraser, S., Chambers, P. J., & Stanley, G. A. (2010). The ethanol stress response and ethanol tolerance of Saccharomyces cerevisiae. *Journal of Applied Microbiology*. https://doi.org/10.1111/j.1365-2672.2009.04657.x
46. Ding, J., Huang, X., Zhang, L., Zhao, N., Yang, D., & Zhang, K. (2009). Tolerance and stress response to ethanol in the yeast Saccharomyces cerevisiae. *Applied Microbiology and Biotechnology*. https://doi.org/10.1007/s00253-009-2223-1
47. Rayman, M. P. (2000). The importance of selenium to human health. *Lancet*. https://doi.org/10.1016/S0140-6736(00)02490-9
48. Zegerman, P., & Diffley, J. F. X. (2009). DNA replication as a target of the DNA damage checkpoint. *DNA Repair*. https://doi.org/10.1016/j.dnarep.2009.04.023
49. Labib, K., & de Piccoli, G. (2011). Surviving chromosome replication: The many roles of the S-phase checkpoint pathway. *Philosophical Transactions of the Royal Society B: Biological Sciences*. https://doi.org/10.1098/rstb.2011.0071
50. Steinbrenner, H., & Sies, H. (2013). Selenium homeostasis and antioxidant selenoproteins in brain: Implications for disorders in the central nervous system. *Archives of Biochemistry and Biophysics*. https://doi.org/10.1016/j.abb.2013.02.021
51. Spallholz, J. E. (1994). On the nature of selenium toxicity and carcinostatic activity. *Free Radical Biology and Medicine*. https://doi.org/10.1016/0891-5849(94)90007-8
52. Tapiero, H., Townsend, D. M., & Tew, K. D. (2003). The antioxidant role of selenium and seleno-compounds. *Biomedicine and Pharmacotherapy*, *57*(3). https://doi.org/10.1016/S0753-3322(03)00035-0
53. Wen, C., He, X., Zhang, J., Liu, G., & Xu, X. (2022). A review on selenium-enriched proteins: preparation, purification, identification, bioavailability, bioactivities and application. *Food and Function*. https://doi.org/10.1039/d1fo03386g
54. Sharma, P., Jha, A. B., Dubey, R. S., & Pessarakli, M. (2012). Reactive Oxygen Species, Oxidative Damage, and Antioxidative Defense Mechanism in Plants under Stressful Conditions. *Journal of Botany*, *2012*. https://doi.org/10.1155/2012/217037
55. Jacob, C., Giles, G. I., Giles, N. M., & Sies, H. (2003). Sulfur and Selenium: The Role of Oxidation State in Protein Structure and Function. *Angewandte Chemie - International Edition*. https://doi.org/10.1002/anie.200300573
56. Letavayová, L., Vlčková, V., & Brozmanová, J. (2006). Selenium: From cancer prevention to DNA damage. *Toxicology*. https://doi.org/10.1016/j.tox.2006.07.017
57. Preda, C., Vasiliu, I., Bredetean, O., Gabriela, C. D., Ungureanu, M. C., Leustean, E. L., … Vulpoi, C. (2016). Selenium in the environment: Essential or toxic to human health? *Environmental Engineering and Management Journal*, *15*(4). https://doi.org/10.30638/eemj.2016.099